

Ejection of hypervelocity stars by the (binary) black hole(s) in the Galactic center

Qingjuan Yu¹ and Scott Tremaine²

¹*Canadian Institute for Theoretical Astrophysics, 60 St. George Street, Toronto, Ontario M5S 3H8, Canada*

²*Princeton University Observatory, Peyton Hall, Princeton, NJ 08544-1001, USA*

ABSTRACT

We study three processes that eject hypervelocity ($> 10^3 \text{ km s}^{-1}$) stars from the Galactic center: (i) close encounters of two single stars; (ii) tidal breakup of binary stars by the central black hole, as originally proposed by Hills; and (iii) three-body interactions between a star and a binary black hole (BBH). Mechanism (i) expels hypervelocity stars to the solar radius at a negligible rate, $\sim 10^{-11} \text{ yr}^{-1}$. Mechanism (ii) expels hypervelocity stars at a rate $\sim 10^{-5}(\eta/0.1) \text{ yr}^{-1}$, where η is the fraction of stars in binaries with semimajor axis $a_b \lesssim 0.3 \text{ AU}$. For solar-mass stars, the corresponding number of hypervelocity stars within the solar radius $R_0 = 8 \text{ kpc}$ is $\sim 60(\eta/0.1)(a_b/0.1 \text{ AU})^{1/2}$. For mechanism (iii), Sgr A* is assumed to be one component of a BBH. We constrain the allowed parameter space (semimajor axis, mass ratio) of the BBH. In the allowed region (for example, semimajor axis of $0.5 \times 10^{-3} \text{ pc}$ and mass ratio of 0.01), the rate of ejecting hypervelocity stars can be as large as $\sim 10^{-4} \text{ yr}^{-1}$ and the expected number of hypervelocity stars within the solar radius can be as large as $\sim 10^3$. Hypervelocity stars may be detectable by the next generation of large-scale optical surveys.

Subject headings: black hole physics – Galaxy: center – stellar dynamics

1. Introduction

The Milky Way, as well as most nearby elliptical galaxies and disk galaxies with spheroids, is believed to house a massive black hole (BH) at its center (e.g. Schödel et al. 2002; Genzel et al. 2003; Schödel et al. 2003; Eisenhauer et al. 2003; Ghez et al. 2003a,b,c; Gebhardt et al. 2003). The deep gravitational potential well close to the BH enables relativistic phenomena, such as the relativistic motion of jets associated with some active galactic nuclei (e.g. Begelman, Blandford & Rees 1984). Hills (1988) first pointed out that stars may also be expelled from

the vicinity of the BH with high velocities. The main features of Hills’ argument can be explained simply. Consider a star with specific energy $E \equiv \frac{1}{2}v^2 + \Phi(r)$, where v and $\Phi(r)$ are the velocity and specific potential of the star at position \mathbf{r} . Close to the BH, $\Phi(r) \simeq -GM_{\bullet}/r$ where G is the gravitational constant and M_{\bullet} is the BH mass. Now suppose that the star approaches close enough to the BH so that $|\Phi(r)| \gg |E|$. In this case, the star will have a velocity $v = \sqrt{2[E - \Phi(r)]} \simeq \sqrt{2GM_{\bullet}/r} = 2.9 \times 10^3 \text{ km s}^{-1} (M_{\bullet}/10^6 M_{\odot})^{1/2} (1 \text{ mpc}/r)^{1/2}$, where $\text{mpc} \equiv 10^{-3} \text{ pc}$ will be often used as a length unit in this paper. If the star then suffers a velocity change $\delta v \ll v$ (e.g. due to interactions with surrounding stars or the tidal disruption of a close binary) and the increase of the specific energy of the star $\delta E = \frac{1}{2}(v + \delta v)^2 - \frac{1}{2}v^2 \simeq v\delta v$ is much larger than $|E|$, the star will escape from the BH with velocity roughly given by

$$\sqrt{2v\delta v} \simeq 1.5 \times 10^3 \text{ km s}^{-1} (M_{\bullet}/10^6 M_{\odot})^{1/4} (1 \text{ mpc}/r)^{1/4} (\delta v/400 \text{ km s}^{-1})^{1/2}. \quad (1)$$

The discovery of such hypervelocity stars—stars with velocity exceeding 10^3 km s^{-1} —would provide strong evidence for the existence of a massive central BH in our Galaxy—if any is still needed—based solely on stellar kinematics in the *outer* parts of the Galaxy. The properties of hypervelocity stars would also illuminate the nature of the innermost regions of galaxies, such as the stellar kinematics, the age and metallicity distribution, the number and mass of the BHs, etc.

In this paper, we will study the expected properties of such hypervelocity stars. We consider three possible scattering processes.

1. Gravitational encounters of single stars. The gravitational interaction of two stars of masses m_i and m_j leads to a velocity change of star m_i ,

$$\begin{aligned} \delta v &= \frac{2Gm_j}{[G^2(m_i + m_j)^2/w_{ij}^2 + Y_{ij}^2 w_{ij}^2]^{1/2}} \\ &\leq \frac{2Gm_j}{[2G(m_i + m_j)Y_{ij}]^{1/2}} \\ &= 4.4 \times 10^2 \text{ km s}^{-1} \left(\frac{2m_j}{m_i + m_j}\right)^{1/2} \left(\frac{m_j}{1 M_{\odot}}\right)^{1/2} \left(\frac{1 R_{\odot}}{Y_{ij}}\right)^{1/2} \end{aligned} \quad (2)$$

where Y_{ij} is the impact parameter and w_{ij} is the initial relative velocity of the two stars (Binney & Tremaine 1987). Only rare close encounters (impact parameters of a few solar radii) can produce velocity changes large enough for a star to escape from the BH at high velocity.

2. Tidal breakup of a binary star. We denote the component masses of the binary as m_1 and m_2 . A binary with semimajor axis a_b will be tidally disrupted by the massive BH

when it passes closer to the BH than the Roche or tidal radius $\sim a_b [M_\bullet / (m_1 + m_2)]^{1/3} \simeq 10 \text{ AU} (a_b / 0.1 \text{ AU}) [M_\bullet / 10^6 (m_1 + m_2)]^{1/3}$. During the tidal breakup, each star will receive a velocity change of order its orbital velocity relative to the center of mass of the binary star, that is, the velocity change of m_1 is about (Hills 1988; Gould & Quillen 2003)

$$\begin{aligned} \delta v &\sim \sqrt{\frac{G(m_1 + m_2)}{a_b}} \left(\frac{m_2}{m_1 + m_2} \right) \\ &\simeq 67 \text{ km s}^{-1} \left(\frac{2m_2}{m_1 + m_2} \right)^{1/2} \left(\frac{m_2}{1 M_\odot} \right)^{1/2} \left(\frac{0.1 \text{ AU}}{a_b} \right)^{1/2}. \end{aligned} \quad (3)$$

If one star gains energy during this process, the other will lose energy and become more tightly bound to the BH. Comparing equations (2) and (3), we see that the semimajor axis of the binary star a_b in equation (3) plays the same role as the impact parameter Y_{ij} in equation (2).

3. Ejection by a binary black hole (BBH). This is actually a special case of mechanism (1), in which the perturbing star m_j is one component of a BBH. The existence of BBHs in some galactic centers is a necessary consequence of hierarchical galaxy formation (Begelman, Blandford & Rees 1980; Yu 2002; Milosavljević & Merritt 2002; Volonteri, Haardt & Madau 2002; Komossa 2003)¹. We denote the component masses of the BBH as M_1 and M_2 ($M_1 \geq M_2$). If the semimajor axis a_\bullet of the BBH is smaller than a certain value $a_h (\equiv GM_2 / 4\sigma_c^2$, where σ_c is the one-dimensional velocity dispersion of the galactic center, see Quinlan 1996, eq. 29), most of the low angular momentum stars that pass through its vicinity will be expelled with an energy gain after one or several close encounters with the BBH, and the average velocity increase of these stars is given by:

$$\delta v \sim F \delta t \sim 1.5 \times 10^3 \text{ km s}^{-1} \left(\frac{2M_2}{M_1 + M_2} \right)^{1/2} \left(\frac{M_2}{10^6 M_\odot} \right)^{1/2} \left(\frac{1 \text{ mpc}}{a_\bullet} \right)^{1/2}, \quad (4)$$

where the force per unit mass from the BH M_2 is $F \sim GM_2 / a_\bullet^2$ and the interaction time $\delta t \sim [G(M_1 + M_2) / a_\bullet^3]^{-1/2}$ (Quinlan 1996). Note that δv in equation (4) is independent of the stellar mass, while δv in equations (2) and (3) depends on the mass of the ejected star; otherwise the three equations have similar form.

This paper is organized as follows. In §2, we review the data on the inner structure of the Galaxy, such as the mass of the central BH, stellar density, etc. In §3, we study the rates

¹We do not consider the possibility of three or more massive BHs in galactic centers, although this configuration may also occur in some galaxies.

of ejecting hypervelocity stars due to the three processes discussed above. A discussion and conclusions are given in §4.

2. The Galactic center

Measurements of stellar radial velocities and proper motions at radii $r \gtrsim 10$ mpc, the discovery of variable X-ray emission around Sagittarius A*, and the tracing of the Keplerian orbits of stars at radii $r \sim 0.1$ – 1 mpc have provided strong evidence for the existence of a massive BH in the center of the Galaxy (Genzel et al. 2000; Baganoff et al. 2001; Schödel et al. 2002; Genzel et al. 2003; Schödel et al. 2003; Eisenhauer et al. 2003; Ghez et al. 2003a,b,c). We expect that the distribution of old stars should be approximately spherical and isotropic, since the two-body relaxation time is short, and this expectation is consistent with the observations (Genzel et al. 2000). We may describe the mass distribution near the center of the Galaxy by the combination of a point mass of $3.5 \times 10^6 M_\odot$ (obtained by averaging the values $(4.0 \pm 0.3) \times 10^6 M_\odot$ in Ghez et al. 2003c and $(2.9 \pm 0.2) \times 10^6 M_\odot$ in Schödel et al. 2003, Fig. 11), plus the visible stellar system with mass density

$$\rho(r) = Ar^{-\alpha} \exp(-r^2/r_b^2). \quad (5)$$

Here $\alpha = 1.8$, the characteristic radius of the bulge is $r_b = 1.9$ kpc, and the normalization A can be obtained by setting $\rho(r = 0.16 \text{ pc}) = 3.6 \times 10^6 M_\odot \text{ pc}^{-3}$ (Dehnen & Binney 1998; Schödel et al. 2003). The density distribution in equation (5) has a cusp at small radii, $\rho \propto r^{-\alpha}$ as $r \rightarrow 0$, consistent with theoretical models of a stellar system with a central BH and all stars having the same mass ($\alpha = 1.75$, e.g. Bahcall & Wolf 1976). At the smallest radii, $r \lesssim 10'' = 0.4 \text{ pc}$, infrared observations suggest that α decreases to 1.4 (Genzel et al. 2003), somewhat below the theoretical models.

Throughout this paper we shall assume that the distance to the Galactic center is $R_0 = 8$ kpc (Eisenhauer et al. 2003). If not otherwise stated, we assume for simplicity that the stars in the Galactic center have the solar mass and radius. The effect of the generalization to a distribution of masses and radii will be discussed briefly in §4.

We define the distribution function (DF) $f(\mathbf{x}, \mathbf{v})$ of a stellar system so that $f(\mathbf{x}, \mathbf{v}) d^3\mathbf{x}d^3\mathbf{v}$ is the number of stars within a phase-space volume $d^3\mathbf{x}d^3\mathbf{v}$ of (\mathbf{x}, \mathbf{v}) . By Jeans’s theorem, the DF in a spherical and isotropic stellar system depends on (\mathbf{x}, \mathbf{v}) only through the specific energy E . The DF $f(E)$ in the Galactic center, which will be used to calculate the ejection rates of hypervelocity stars below, can be obtained from equation (5) and the Edington formula (eq. 4-140a in Binney & Tremaine 1987). The potential in the stellar system $\Phi(r) = \Phi_\bullet(r) + \Phi_*(r)$ is contributed by both the central BH (Φ_\bullet) and the bulge stars (Φ_*);

however, at small radii $r \lesssim 1$ pc the gravitational potential contributed by stars can be ignored. In this region we have $\Phi = \Phi_\bullet = -GM_\bullet/r$, $\rho(r) \propto r^{-\alpha}$, and the stellar DF is

$$f(E) = C|E|^{\alpha-3/2}, \quad (6)$$

where

$$C = 2^{-3/2}\pi^{-3/2} \frac{\Gamma(1+\alpha)}{\Gamma(\alpha-\frac{1}{2})} \cdot \frac{\rho(r)}{m_*} \sigma(r)^{-2\alpha}, \quad \sigma(r) \equiv \sqrt{\frac{GM_\bullet}{r}}, \quad (7)$$

and m_* is the stellar mass. Note that C is independent of radius since the radial variations of $\rho(r)$ and $\sigma(r)$ cancel.

3. Rates of ejecting stars with high velocities

In this section, we study the rates of ejecting stars with high velocities from the Galactic center. We will consider in turn the three ejection mechanisms described in §1.

3.1. Close encounters between two single stars

Two-body gravitational encounters between single stars can eject one of the two stars (Hénon 1969; Lin & Tremaine 1980). Consider a test star with mass m_i and velocity \mathbf{v}_i that encounters a star with velocity \mathbf{v}_j . The test star will experience a velocity change from \mathbf{v}_i to $\mathbf{v}_i + \mathbf{e}_{ij}$ (see eq. 2 for $|\mathbf{e}_{ij}|$). If the test star is moving through a background of stars with DF $f(\mathbf{r}, \mathbf{v})$, the probability that this star will suffer an encounter with a background star during time dt , $\Gamma_i(\mathbf{r}, \mathbf{v}_i)dt$, is given by:

$$\Gamma_i(\mathbf{r}, \mathbf{v}_i)dt = dt \int d^3\mathbf{v}_j f(\mathbf{r}, \mathbf{v}_j) w_{ij} \int dY_{ij}^2 \int d\Psi_{ij}, \quad (8)$$

where Y_{ij} is the impact parameter, $w_{ij} = |\mathbf{v}_i - \mathbf{v}_j|$ is the relative velocity and Ψ_{ij} is the angle between the $(\mathbf{v}_i, \mathbf{v}_j)$ plane and the $(\mathbf{v}_i - \mathbf{v}_j, \mathbf{e}_{ij})$ plane (Hénon 1960). If the velocity distribution of field stars is isotropic, we have

$$\Gamma_i(\mathbf{r}, \mathbf{v}_i)dt = dt \int dv_j \frac{2\pi v_j}{v_i} f(\mathbf{r}, v_j) \int dw_{ij} w_{ij}^2 \int dY_{ij}^2 \int d\Psi_{ij}, \quad (9)$$

where $v_j = |\mathbf{v}_j|$. The probability that the test star is expelled with a velocity higher than v_0 at infinity can be obtained by restricting this integral to the encounters that change the value of its velocity from $v_i = |\mathbf{v}_i|$ to a value larger than v_e , i.e.,

$$|\mathbf{v}_i + \mathbf{e}_{ij}| \geq v_e. \quad (10)$$

Here $\frac{1}{2}v_0^2 + \Phi(r = \infty) = \frac{1}{2}v_e^2 + \Phi(r) \equiv E_0$, and we shall assume that $\Phi(r = \infty) = 0$. We call v_0 the ejection speed and E_0 the ejection energy. Thus, the rate of ejecting stars with ejection speed higher than v_0 due to two-body encounters in a unit volume around position \mathbf{r} , $\mathcal{R}(\mathbf{r}, v_0)$, is given by:

$$\begin{aligned} \mathcal{R}(\mathbf{r}, v_0) &= \int d^3\mathbf{v}_i f(\mathbf{r}, \mathbf{v}_i) \Gamma_i(\mathbf{r}, \mathbf{v}_i) \\ &= 8\pi^2 \int dv_i \int dv_j \int dw_{ij} \int dY_{ij}^2 \int d\Psi_{ij} f(\mathbf{r}, v_i) f(\mathbf{r}, v_j) v_i v_j w_{ij}^2, \end{aligned} \quad (11)$$

where the integration variables should satisfy the inequality (10). The total rate of ejecting stars with ejection speed higher than v_0 is given by

$$\frac{dN_{\text{ej}}(v_0)}{dt} = 4\pi \int_0^\infty \mathcal{R}(\mathbf{r}, v_0) r^2 dr. \quad (12)$$

The ejection rate can be obtained analytically in some cases. Ignoring possible stellar collisions (when the impact parameter Y_{ij} is small enough) and treating stars as point masses with zero radius, equation (11) can be simplified as follows (Hénon 1969; Lin & Tremaine 1980):

$$\mathcal{R}(\mathbf{r}, v_0) = \frac{2^{13/2}}{3} \pi^3 G^2 m_*^2 \int_\Phi^0 dE f(E) \int_{E_0 + \Phi - E}^0 dE' f(E') \frac{(E' + E - E_0 - \Phi)^{3/2}}{(E_0 - E)^2}. \quad (13)$$

By ignoring the gravitational potential contributed by stars (e.g. in the region close to the BH) and applying equation (6) in equations (12) and (13), the total ejection rate of stars as a function of ejection speed can be found to be (Lin & Tremaine 1980):

$$\frac{dN_{\text{ej}}(v_\bullet)}{dt} = \frac{2^{5/2} \pi^{3/2} G^5 M_\bullet^3 \rho^2}{3 \sigma^9} \left(\frac{E_\bullet}{\sigma^2} \right)^{2\alpha - 9/2} \frac{\Gamma^2(1 + \alpha) \Gamma(\frac{9}{2} - 2\alpha)}{(3 - \alpha)(2 - \alpha)}. \quad (14)$$

Although the ejection rate in this equation is integrated over radius, we have expressed it in terms of the velocity dispersion $\sigma(r)$ and the density $\rho(r)$, given by equation (7)—these can be evaluated at any radius since their radial dependences cancel out in equation (14). Note that in this formula the ejection speed v_\bullet represents the velocity after escaping the gravity of the central BH but before climbing through the bulge, and the ejection energy $E_\bullet = \frac{1}{2}v_\bullet^2$. Using $\alpha = 1.8$, BH mass $M_\bullet = 3.5 \times 10^6 M_\odot$, and the stellar mass density distribution $\rho(r) = Ar^{-\alpha}$ (see eq. 5 and the subsequent text) in equation (14), we obtain the ejection rate shown in Figure 1 as the dotted line at the top of the figure.

In reality, stars have non-zero radii, and encounters of two stars with impact parameter $Y_{ij} < Y_{\text{coll}} \equiv (R_i + R_j)[1 + 2G(m_i + m_j)/(R_i + R_j)w_{ij}^2]^{1/2}$ will lead to stellar collisions, where

R_i and R_j are the radii of the two stars m_i and m_j . Such collisions have two principal effects on the calculation of the ejection rate: (i) Encounters with $Y_{ij} < Y_{\text{coll}}$ should not be included in equation (11). (ii) Stars cannot diffuse to energies $E \lesssim -Gm_*/R_*$ without colliding first, where R_* is the stellar radius (Bahcall & Wolf 1976). Thus, we cut off the stellar distribution, so that $f(E) = 0$ for $E < -Gm_*/R_*$. After making these modifications, the ejection rate is hard to obtain analytically so we resort to numerical calculations, shown by the dashed line in Figure 1. As seen from Figure 1, the ejection rate is significantly decreased by stellar collisions, especially at speeds $\gtrsim 300 \text{ km s}^{-1}$ that approach or exceed the escape speeds from the stellar surface.

These results do not include the effects of the gravitational potential of the bulge, disk and halo. To include the effects of the bulge, we use equation (5) to compute the gravitational potential from the bulge; we add the potential from the BH and use Eddington’s formula to compute the bulge DF $f(E)$; we then truncate the DF for $E - \Phi_*(r=0) < -Gm_*/R_*$, and insert the result into the formula (13) to obtain the ejection rate. The result is shown by the bold solid line in Figure 1; this is much lower than the dashed line at low speeds, because low-velocity stars cannot climb the potential to escape the stellar bulge. The difference between the bold solid line and the dashed line is negligible at ejection speeds higher than 1000 km s^{-1} .

These results do not include the potential of the Galactic disk and halo. The gravitational potential difference between $R_0 = 8 \text{ kpc}$ and the outer parts of the bulge, $r_b \simeq 2 \text{ kpc}$, can be roughly estimated by

$$\Delta\Phi = V_c^2 \ln(R_0/r_b) \simeq \frac{1}{2}(370 \text{ km s}^{-1})^2 (V_c/220 \text{ km s}^{-1})^2, \quad (15)$$

where V_c is the circular speed, assumed independent of radius. The velocity distribution of the stars that reach the solar radius R_0 is given by

$$v_h = \sqrt{v_0^2 - 2\Delta\Phi}. \quad (16)$$

The thin solid line in Figure 1 shows the ejection rate as a function of v_h , which is obtained from the bold solid line using equations (15) and (16).

The ejection rate of stars at speeds $> 100 \text{ km s}^{-1}$ is about $(1-2) \times 10^{-8} \text{ yr}^{-1}$ at the outer edge of the bulge and about $2 \times 10^{-9} \text{ yr}^{-1}$ at the solar radius; the ejection rate of stars at speeds $> 500 \text{ km s}^{-1}$ is only 10^{-9} yr^{-1} at the edge of the bulge and a factor of three lower at the solar radius; and the ejection rate at speeds $> 1000 \text{ km s}^{-1}$ is only 10^{-11} yr^{-1} at either location. We conclude that the expected rate of formation of hypervelocity stars in the Galaxy due to two-body close encounters of single stars is negligible.

Finally, to illustrate the importance of the BH, we show the ejection rate from a stellar system with the same density distribution as that in the Galactic center but without a central BH (the dot-dashed line in Figure 1). The existence of a central BH dramatically increases the rate of ejecting hypervelocity stars.

3.2. Tidal breakup of a binary star by the central BH

It is plausible that binary stars are formed as commonly near the Galactic center as they are in the solar neighborhood. Close encounters between a close binary and a massive BH may break up the binary through an exchange collision, in which one binary component becomes bound to the BH and the other is ejected at high velocity (up to several thousand km s^{-1} ; Hills 1988; Gould & Quillen 2003).

We shall focus on binaries in the semimajor axis range $0.01 \text{ AU} < a_b < 0.3 \text{ AU}$; 0.01 AU is nearly $2R_\odot$ and thus is a lower limit to the binary separation for solar-type stars, and the choice of an upper limit of 0.3 AU will be explained later. The binary period distribution observed locally by Duquennoy & Mayor (1991) implies that roughly 8% of binaries belong to this period range; given that the fraction of stars in binaries is ~ 0.5 we expect that the binary fraction in the semimajor axis range $0.01 \text{ AU} < a_b < 0.3 \text{ AU}$ is about 0.04. This estimate is quite uncertain, both because the estimate derived for the solar neighborhood is uncertain and because we do not know whether the binary distribution is the same at the Galactic center as it is in the solar neighborhood.

We must first check that these binaries are not disrupted by encounters with single stars. The disruption time is (Binney & Tremaine 1987)

$$t_{\text{dis}} = 0.1 \frac{\sigma}{G\rho a_b \ln \Lambda}, \quad (17)$$

where ρ is the density of stars (eq. 5), a_b is the semimajor axis of the binary, σ is the velocity dispersion, $\ln \Lambda$ is the Coulomb logarithm, and we have assumed that the binary components and the field stars have the same mass. In the region $r \lesssim 1 \text{ pc}$ where the gravitational potential is dominated by the BH, we may take $\sigma \simeq (GM_\bullet/r)^{1/2}$ and $\Lambda \simeq (M_\bullet/m_*)(a_b/r)$, so that

$$t_{\text{dis}} = \frac{4 \times 10^{10} \text{ yr}}{\ln[1.7(a_b/0.1 \text{ AU})(1 \text{ pc}/r)]} \left(\frac{r}{1 \text{ pc}} \right)^{1.3} \left(\frac{0.1 \text{ AU}}{a_b} \right). \quad (18)$$

This formula is derived for soft binaries, for which $\Lambda \gtrsim 1$; a similar result holds for hard binaries, except that $\ln \Lambda$ is replaced by unity, and t_{dis} represents the timescale in which the semimajor axis shrinks by a factor of two due to encounters. We conclude that binaries with

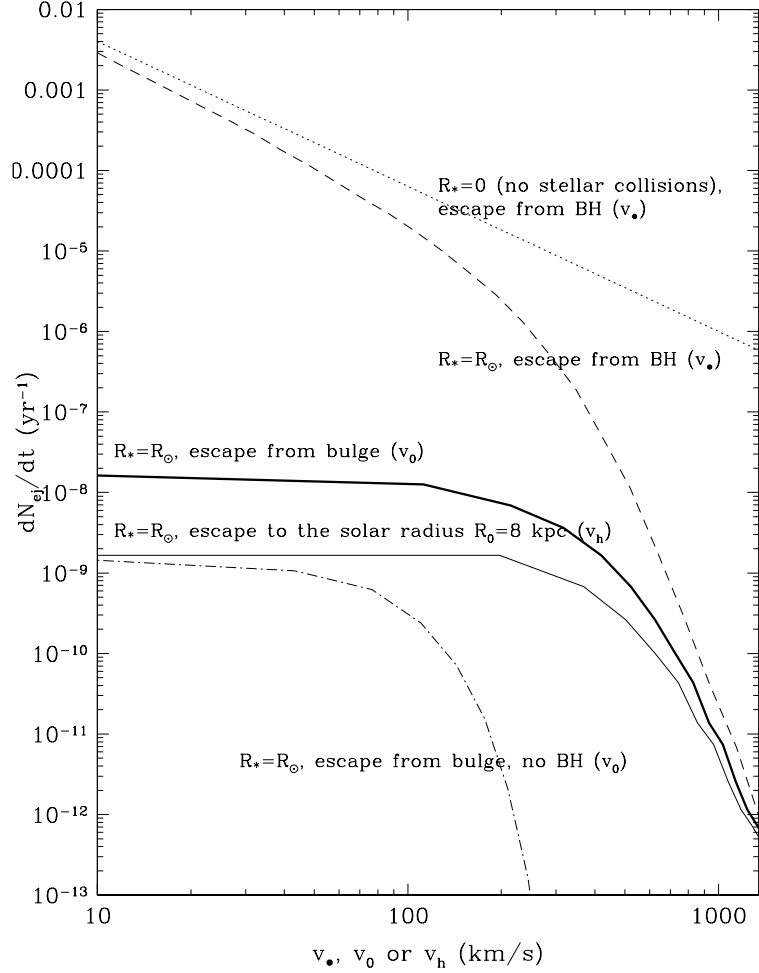


Fig. 1.— Estimated rates of ejecting stars from the Galactic center by two-body encounters of single stars. Here v_* is the velocity after escaping from the BH, v_0 is the velocity after escaping from the bulge, and v_h is the velocity after reaching the solar radius. The dotted line (a function of v_*) is obtained by treating stars as point masses with zero stellar radius and ignoring the gravitational potential contributed by bulge stars (see eq. 14). The dashed line (a function of v_*) is obtained by assuming that all stars have the solar radius. The bold solid line (a function of v_0) is the ejection rate including the effects of both non-zero stellar radii and the gravitational potential of the bulge. The thin solid line (a function of v_h) is the rate at which ejected stars reach the solar radius (see eqs. 15 and 16). The current of hypervelocity stars with velocity $> 700 \text{ km s}^{-1}$ past the solar radius is negligible (less than 1 per Hubble time). The dot-dashed line is the ejection rate including the effects of both non-zero stellar radii and the gravitational potential of the bulge, but assuming that there is no central BH. The existence of the BH increases the ejection rate, especially at high velocities.

semimajor axis $a_b = 0.3 \text{ AU}$ can survive for the age of the Galaxy outside $r \simeq 0.8 \text{ pc}$, while binaries with $a_b = 0.01 \text{ AU}$ can survive outside $r \sim 0.05 \text{ pc}$.

We now review Hills’ (1988) three-body simulations of the encounter between a binary and a massive BH. The center of mass of the binary is initially on an unbound orbit relative to the BH, with velocity v_∞ . The probability of an exchange collision is a decreasing function of the dimensionless closest-approach parameter

$$R'_{\min} \equiv \frac{R_{\min}}{a_b} \left(\frac{M_\bullet}{m_*} \right)^{-1/3}; \quad (19)$$

here we have assumed for simplicity that $m_1 = m_2 = m_*$, and R_{\min} is the closest approach of the binary to the BH (the periapsis of the orbit of the center of mass of the binary around the BH). The parameter R'_{\min} is essentially the distance of closest approach in units of the Roche radius of the binary. Hills finds that exchange collisions occur in nearly 80% of encounters with $R'_{\min} \simeq 0.3$ and in 50% of encounters with $R'_{\min} \simeq 1$. Let us define an ejection speed parameter by (eqs. 1 and 3)

$$v'_\bullet \equiv v_\bullet \left(\frac{m_*}{M_\bullet} \right)^{1/6} \left(\frac{a_b}{0.1 \text{ AU}} \cdot \frac{M_\odot}{m_*} \right)^{1/2}, \quad (20)$$

where v_\bullet is the rms velocity at infinity of the ejected star. Then v'_\bullet is mainly a function of R'_{\min} , and roughly independent of the BH mass and the semimajor axis and masses of the binary components. The velocity v'_\bullet varies between 130 and 160 km s^{-1} for $R'_{\min} = 0-1$, with a peak near $R'_{\min} \simeq 0.3$, and is about 130 km s^{-1} at $R'_{\min} = 1$ (Hills 1988).

These results are independent of the initial relative velocity v_∞ of the binary relative to the BH. This assumption is correct so long as this is much less than the relative velocity at R_{\min} , which in turn requires that²

$$v_\infty \lesssim \left(\frac{Gm_*}{a_b} \right)^{1/2} \left(\frac{M_\bullet}{m_*} \right)^{1/3}. \quad (21)$$

For the Galaxy this limit corresponds to $v_\infty \lesssim 1.4 \times 10^4 \text{ km s}^{-1} (0.1 \text{ AU}/a_b)^{1/2}$, which is satisfied by a large margin. Similarly, Hills’ results for the probability of an exchange collision should be valid for orbits that are bound to the BH so long as the orbits are very eccentric, that is, $R_{\min} \ll a$ where a is the semimajor axis of the orbit around the BH.

²The dependence of the exchange cross-section on v_∞ is mapped out in more extensive three-body integrations by Hills (1991), although Hills’ empirical summary of the results is based on the assumption that the critical velocity scales as $M_\bullet^{1/6}$, not $M_\bullet^{1/3}$ as in equation (21).

For numerical estimates we assume that both binary components have the solar mass. According to equation (19), for a binary to have an exchange probability of 50% or more in an encounter with a $3.5 \times 10^6 M_\odot$ BH, it must pass within about $R_{\min} \simeq 150a_b$ of the BH; that is, within $R_{\min} = 1.5$ or 45 AU for $a_b = 0.01$ and 0.3 AU respectively. The rms ejection speed at infinity v_\bullet in this case is about 5×10^3 or $0.9 \times 10^3 \text{ km s}^{-1}$ for $a_b=0.01$ or 0.3 AU respectively. These ejection speeds for $a_b \lesssim 0.3$ AU are high enough to escape the Galactic bulge and even the Galactic halo, which is why we restrict our attention to this range of binary semimajor axis.

The ejection rate depends on the flux of binary stars passing close to the central BH, specifically, within a periapsis distance $R_{\min} \simeq 150a_b$. The region in the (J, E) = (specific angular momentum, specific energy) phase space where a binary star has dimensionless closest approach parameter $R'_{\min} \lesssim 1$ is called the “loss cone” and is given by:

$$J^2 \leq J_{\text{lc}}^2(E, a_b) \equiv 2R_{\min}^2 [E - \Phi(R_{\min})] \simeq 2GM_\bullet R_{\min} \quad (|E| \ll GM_\bullet/R_{\min}). \quad (22)$$

[Note that the concept of the “loss cone” is used in other contexts, for example, see Magorrian & Tremaine (1999) for the tidal disruption of single stars by a massive BH or Yu (2002) and §3.3 for the expulsion of low-angular momentum stars by a BBH. The loss cone for disruption of single stars is usually much smaller than the loss cone for disruption of binary stars.] At first, the ejection rate is determined by the rate of depletion of the initial population of binary stars in the loss cone, and the rate per unit energy is given by (see eq. 19 in Yu 2002):

$$F^{\text{full}}(E, a_b) \simeq 4\pi^2 \eta f(E) J_{\text{lc}}^2(E, a_b), \quad t \lesssim P(E), \quad (23)$$

where $P(E)$ is the radial period of an orbit with energy E and zero angular momentum, and η is the number fraction of binary stars. As the binary stars in the loss cone are disrupted, new binaries are scattered into the loss cone by two-body relaxation. Eventually, the scattering into the loss cone reaches a steady state. The steady-state diffusion rate of binary stars into the loss cone per unit energy is obtained from the Fokker-Planck equation (eq. 24 in Magorrian & Tremaine 1999):

$$F_{\text{lc}}(E) \simeq \begin{cases} qF^{\text{full}}(E, a_b)/\ln[GM_\bullet/(4|E|R_{\min})], & \text{if } q \ll -\ln(J_{\text{lc}}^2/J_c^2) \\ F^{\text{full}}(E, a_b), & \text{if } q \gg -\ln(J_{\text{lc}}^2/J_c^2) \end{cases}, \quad (24)$$

where

$$q \equiv P(E) \bar{\mu}(E) J_c^2(E) / J_{\text{lc}}^2(E, a_b). \quad (25)$$

Here $\bar{\mu}$ is the orbit-averaged diffusion coefficient and $J_c^2(E)$ is the specific angular momentum of a circular orbit at energy E . The quantity $\frac{1}{2}qJ_{\text{lc}}^2$ is the mean-square change in the scalar angular momentum for a nearly radial orbit in one orbital period; $\frac{1}{2}qJ_{\text{lc}}^2 = P(E) \langle (\Delta J)^2 \rangle =$

$P(E)\langle r^2(\Delta v_t)^2 \rangle$, where $\langle \cdot \rangle$ denotes an orbit-averaged diffusion coefficient and v_t is the tangential velocity (see details in Appendix B of Magorrian & Tremaine 1999). The region in which $q \gtrsim -\ln(J_{lc}^2/J_c^2)$ is known as the “pinhole” or “full loss cone” regime, as opposed to the “diffusion” or “empty loss cone” regime. Generally the loss cone is full at large radii and empty at small radii, we shall define the critical radius r_{crit} to be the apoapsis of orbits at the transition between these two regimes. The critical radius $r_{\text{crit}} \sim 600$ pc for $a_b = 0.3$ AU and ~ 20 pc for $a_b = 0.01$ AU.

We can use the model for the Galactic center described in §2 to estimate the ejection rate due to disruption of binary stars. As usual we assume that the DF is isotropic in velocity space, and that it vanishes for energy $E - \Phi_*(r=0) \simeq E < -GM_\odot/R_\odot$ (without this cutoff the ejection rate for a full loss cone diverges). If the binary loss cone is full, the ejection rate is given by equation (23):

$$\begin{aligned} n_{\text{ej}} &= \int F^{\text{full}}(E) dE \\ &\simeq 8\pi^2 \eta GM_\bullet R_{\text{min}} C \int_{-GM_\odot/R_\odot}^0 |E|^{\alpha-3/2} dE \\ &\simeq 2 \times 10^{-2} \text{ yr}^{-1} \left(\frac{\eta}{0.1} \right) \left(\frac{a_b}{0.1 \text{ AU}} \right) \left(\frac{R'_{\text{min}}}{1} \right) \left(\frac{M_\bullet}{3.5 \times 10^6 M_\odot} \right)^{4/3-\alpha}, \end{aligned} \quad (26)$$

which is approximately consistent with the estimate $\sim 10^{-2}(\eta/0.1)(a_b/0.1 \text{ AU})$ in Hills (1988), based on much less certain observational parameters. However, this calculation, like Hills’, neglects the fact that the binaries initially in the loss cone are rapidly depleted. For a more accurate ejection rate we must use equation (24), which yields

$$n_{\text{ej}} = \int F_{lc}(E) dE \simeq 1.5 \times 10^{-5} (\eta/0.1) \text{ yr}^{-1} \quad (27)$$

if $a_b = 0.3$ AU. The ejection rate is quite insensitive to the binary semimajor axis a_b , decreasing to only $n_{\text{ej}} = 0.9 \times 10^{-5} (\eta/0.1) \text{ yr}^{-1}$ if $a_b = 0.01$ AU. The apoapsides of most of the stars contributing to the total diffusion rate into the loss cone are in the range 2–3 pc for $a_b = 0.01$ –0.3 AU; at these radii the binary disruption rate due to encounters with field stars (eq. 18) is small. Because the loss cone is not full, Hills’ simple estimate of the ejection rate is too large by three orders of magnitude at $a_b = 0.1$ AU.

The time required for the ejected stars to travel a distance D is by:

$$\begin{aligned} t_D &\simeq \frac{D}{v_\bullet} = 5 \times 10^6 \text{ yr} \left(\frac{D}{8 \text{ kpc}} \cdot \frac{1.6 \times 10^3 \text{ km s}^{-1}}{v_\bullet} \right) \\ &\sim 5 \times 10^6 \text{ yr} \left(\frac{D}{8 \text{ kpc}} \cdot \frac{1.3 \times 10^2 \text{ km s}^{-1}}{v'_\bullet} \right) \end{aligned} \quad (28)$$

$$\times \left(\frac{3.5 \times 10^6 M_\odot}{M_\bullet} \cdot \frac{m_*}{M_\odot} \right)^{1/6} \left(\frac{a_b}{0.1 \text{ AU}} \cdot \frac{M_\odot}{m_*} \right)^{1/2}, \quad (29)$$

where v'_\bullet is the ejection speed parameter defined in equation (20). From equations (27) and (29), the number of hypervelocity stars inside the sphere with radius D is given by:

$$n_{\text{ej}} t_{\text{D}} \sim 60 \left(\frac{\eta}{0.1} \right) \left(\frac{D}{8 \text{ kpc}} \right) \left(\frac{a_b}{0.1 \text{ AU}} \right)^{1/2} \left(\frac{M_\odot}{m_*} \right)^{1/3}. \quad (30)$$

In this process, one component of the binary star is ejected with an energy gain, and the other loses energy and becomes more tightly bound to the BH. The apoapsis distance of the bound star is approximately $GM_\bullet/v_\bullet^2 \simeq 1 \times 10^3 \text{ AU} (M_\bullet/3.5 \times 10^6 M_\odot) (1.6 \times 10^3 \text{ km s}^{-1}/v_\bullet)^2$. The eccentricity of the bound star is usually high, and the corresponding orbital period is $\sim 8 \text{ yr} (M_\bullet/3.5 \times 10^6 M_\odot) (1.6 \times 10^3 \text{ km s}^{-1}/v_\bullet)^3$. Recent high-resolution infrared observations of the region around the compact radio source (and presumed BH) Sgr A* have revealed massive young stars on high-eccentricity orbits with periods of decades or less (Schödel et al. 2002, 2003; Eisenhauer et al. 2003; Ghez et al. 2003a,b,c). Gould & Quillen (2003) have suggested that these unusual orbits may have been produced by Hills’ mechanism; that is, these stars may be one component of a tidally disrupted binary star. According to equation (27), we expect that the number of young (10^7 yr old) stars that are the remnants of tidally disrupted binaries should be $\sim 100(\eta/0.1)$ at any time. Of course, the number of high-mass remnants would be smaller, by an amount that depends on the shape of the initial mass function.

3.3. Interactions between a single star and a massive BBH

BBHs are likely to exist in some galactic centers (Begelman, Blandford & Rees 1980; Yu 2002), and perhaps in the Galactic center as well. In fact, Hansen & Milosavljević (2003) have recently argued that the young stars observed at 0.1–1 mpc distances from Sgr A* may have been shorn from a disk or cluster surrounding the smaller component of a BBH, by tidal forces from the larger component. A massive BBH steadily loses orbital energy to the surrounding stellar population. When the two BHs are orbiting independently in the galaxy, and even after they form a bound binary system, the energy loss is mainly through dynamical friction. Once the BBH becomes sufficiently tightly bound that its orbital velocity exceeds the velocity dispersion of the stars, dynamical friction becomes less and less effective, and three-body interactions with low-angular momentum stars passing through the BBH become the dominant energy-loss mechanism. When the BBH becomes “hard”, at a semimajor axis

(Quinlan 1996)

$$a_h \equiv \frac{GM_2}{4\sigma_c^2} \simeq 0.04 \text{ pc} \left(\frac{\nu}{0.1} \right) \left(\frac{M_1 + M_2}{3.5 \times 10^6 M_\odot} \right) \left(\frac{100 \text{ km s}^{-1}}{\sigma_c} \right)^2, \quad (31)$$

where

$$\nu \equiv M_2/(M_1 + M_2) \quad (32)$$

is the mass ratio of the small BH to the BBH, most of the low-angular momentum stars that pass near a BBH will eventually be expelled with an energy gain after one or several encounters with the BBH. In such expulsions, the average ejection speed of the stars is

$$v_\bullet \simeq \sqrt{\frac{3.2GM_1M_2}{(M_1 + M_2)a_\bullet}} \simeq 2.2 \times 10^3 \text{ km s}^{-1} \left(\frac{\nu}{0.1} \right)^{1/2} \left(\frac{1 \text{ mpc}}{a_\bullet} \right)^{1/2} \left(\frac{M_1}{3.5 \times 10^6 M_\odot} \right)^{1/2} \quad (33)$$

(see eq. 17 in Yu 2002). The average relative energy change $\Delta\mathcal{E}/\mathcal{E}$ per ejection is independent of the BBH orbital energy \mathcal{E} . As the semimajor axis of the BBH continues to decrease, eventually gravitational radiation takes over as the dominant energy loss mechanism.

We now ask what are the observational constraints on the mass ratio ν and semimajor axis a_\bullet of a possible BBH in the Galactic center. We shall assume that the total mass $M_1 + M_2 = 3.5 \times 10^6 M_\odot$, that the BBH is on a circular orbit, and that Sgr A* is the larger component M_1 of the BBH. (We shall argue below that Sgr A* is unlikely to be the small component of the BBH.) For reference, the orbital period of the BBH is

$$P_{\text{BBH}} = \frac{2\pi a_\bullet^{3/2}}{\sqrt{G(M_1 + M_2)}} \simeq 1.6 \text{ yr} \left(\frac{a_\bullet}{1 \text{ mpc}} \right)^{3/2} \left(\frac{3.5 \times 10^6 M_\odot}{M_1 + M_2} \right)^{1/2} \quad (34)$$

There are several constraints on the properties of the BBH:

- A census of stars within $\sim 10'' \simeq 0.4 \text{ pc}$ of the Galactic center reveals that the peak of the stellar surface density agrees with the position of Sgr A* within $\sim 0''.2 \simeq 8 \text{ mpc}$ (Genzel et al. 2003). Taking the center of mass of the BBH as the center of the stellar distribution, and ignoring the small possibility that the two BHs are aligned along the line of sight to us, we have the following constraint on the distance between Sgr A* and the center of mass of the BBH:

$$\nu a_\bullet \lesssim 0''.2 \simeq 8 \text{ mpc}. \quad (35)$$

In panel (b) of Figure 2, the region below the bold long-dashed line gives the parameter space represented by inequality (35).

- The eccentric Keplerian orbits of stars at radii $r \sim 0.1\text{--}1$ mpc (Schödel et al. 2002, 2003; Ghez et al. 2003a,b,c) will eventually provide strong constraints on the properties of a BBH at the Galactic center. However, a binary with semimajor axis small compared to the periapsis distance of the stellar orbit, or large compared to the apoapsis distance, will be poorly constrained because the orbit will be nearly a Keplerian ellipse, with one focus at either the center of mass or one component of the BBH, respectively. Moreover, so far these stars have only been observed for a fraction of an orbital period, so the sensitivity to deviations from a Keplerian orbit is still relatively small (but growing rapidly). Without carrying out proper simulations, we guess that the agreement of the observations to date with orbits around a single point mass constrains the mass fraction to be $\nu \lesssim 0.2$ if a_\bullet is in the range $\sim 0.1\text{--}1$ mpc. According to this constraint, the BBH is unlikely to be in the box enclosed by the dot-long-dashed line near the right boundary of panel (b) of Figure 2.
- Observations of the proper motion of Sgr A* also constrain the parameter space (a_\bullet, ν) of a putative BBH in the Galactic center. VLBA observations from 1995 to 2000 show that the dominant term in the proper motion of Sgr A* with respect to extragalactic radio sources comes from the motion of the Sun around the Galactic center. The rms residual from uniform motion is $\Delta \simeq 0.5$ mas = 0.02 mpc, and the upper limit of the peculiar motion of Sgr A* perpendicular to the Galactic plane is $v_\perp \simeq 8$ km s⁻¹ (Backer & Sramek 1999; Reid et al. 1999, 2003). We do not know the motion of the Sun in the Galactic plane with comparable accuracy, but unless the peculiar velocity of Sgr A* happens to be closely aligned with the Galactic plane, it is unlikely to be larger than $\sqrt{2}v_\perp \simeq v_{\max} \simeq 12$ km s⁻¹. If the orbital period of the BBH P_{BBH} (eq. 34) is short compared to the observation interval $T = 5$ yr, then the amplitude of the motion of Sgr A* relative to the center of mass of the BBH must be smaller than the rms observational error, that is,

$$\nu a_\bullet \lesssim f \Delta, \tag{36}$$

where f is of order unity. In the opposite limit, if $P_{\text{BBH}} \gg T$ then the velocity of Sgr A* relative to the center of mass must be less than v_{\max} , so

$$\nu a_\bullet \lesssim f v_{\max} P_{\text{BBH}} / (2\pi). \tag{37}$$

We set $f \simeq 2$ and simply choose the transition between inequalities (36) and (37) so that they are continuous. In panel (b) of Figure 2, the region on the left side of the bold solid line gives the parameter space allowed by inequalities (36) and (37) with $\Delta = 0.5$ mas and $v_{\max} = 12$ km s⁻¹ (Reid et al. 2003).

The rate of ejecting stars by interactions with a hard BBH depends on the flux of low angular momentum stars passing through the vicinity of the BBH. Just as in the case of the

loss cone of binary stars discussed in §3.2, here the region in the (specific energy, specific angular momentum) phase space in which a star can pass within $\sim a_\bullet$ of the BBH is called the loss cone, and may be found by replacing R_{\min} with the semimajor axis of the BBH in equation (22) (see Yu 2002). Initially, the loss cone of the BBH is full. As stars are removed from the loss cone by close encounters with the BBH, new stars refill the loss cone by two-body relaxation (or by non-axisymmetric gravitational forces from the surrounding stellar system, if it is non-spherical; see Yu 2002). Eventually the system reaches a steady state controlled by the balance between the ejection rate of stars and the rate at which stars refill the loss cone. If the rms angular momentum transferred to or from the stars per orbital period is larger than J_{lc} (see eq. 22), then the stars will refill the loss cone as fast as it is depleted and the loss cone remains full; otherwise, the stars will slowly diffuse into the loss cone and the loss cone remains nearly empty. The refilling rate due to two-body relaxation can be found by solving the steady-state Fokker-Planck equation (e.g. eq. 17 in Magorrian & Tremaine 1999 or see Yu 2002). If the BBH is hard and has a total mass $3.5 \times 10^6 M_\odot$, our calculations show that the rate of removing stars from the loss cone is $n_{\text{BBH}}^{\text{full}} \simeq 2 \text{ yr}^{-1} (a_\bullet / 1 \text{ mpc})$ when the loss cone is full and $n_{\text{BBH}}^{\text{diff}} \simeq (1-3) \times 10^{-4} \text{ yr}^{-1}$ when the loss cone is empty; the superscript “diff” refers to the fact that the refilling of the loss cone is a diffusive process. The rate $n_{\text{BBH}}^{\text{full}}$ is insensitive to the BBH mass ratio ν , and the rate $n_{\text{BBH}}^{\text{diff}}$ is insensitive to both a_\bullet (only through the logarithmic term in eq. 24) and ν , so long as the BBH is hard and the mass of the smaller component of the BBH is significantly larger than the stellar mass (Quinlan’s 1996 simulations only cover the range $\nu > 0.004$ but his finding that the hardening is largely independent of ν should extend to more extreme mass ratios). The hardening timescale of the BBH is then given by (see eq. 33):

$$t_h(a_\bullet) = \left| \frac{a_\bullet}{\dot{a}_\bullet} \right| \simeq \frac{M_1 + M_2}{3m_* n_{\text{BBH}}^{\text{diff}}} \simeq 6 \times 10^9 \text{ yr} \left(\frac{M_1 + M_2}{3.5 \times 10^6 M_\odot} \right) \left(\frac{1 M_\odot}{m_*} \right) \left(\frac{2 \times 10^{-4} \text{ yr}^{-1}}{n_{\text{BBH}}^{\text{diff}}} \right), \quad (38)$$

which is shown as a function of a_\bullet and ν in Figure 2 (see the solid horizontal lines in panels c and d, which represent $4, 6, 8 \times 10^9 \text{ yr}$ from top to bottom). Assuming that the BBH orbit is circular, its gravitational radiation timescale is given by (Peters 1964):

$$t_{\text{gr}}(a_\bullet, \nu) = \left| \frac{a_\bullet}{\dot{a}_\bullet} \right| = \frac{5}{64} \frac{c^5 a_\bullet^4}{G^3 M_1 M_2 (M_1 + M_2)} \simeq 5.4 \times 10^8 \text{ yr} \left(\frac{a_\bullet}{1 \text{ mpc}} \right)^4 \frac{(3.5 \times 10^6 M_\odot)^3}{(M_1 + M_2)^2 M_1} \left(\frac{0.1}{\nu} \right), \quad (39)$$

which is also shown in panels (c) and (d) of Figure 2 (the long-dashed lines, which represent $10^9, 10^8, 10^7 \text{ yr}$ from top to bottom). A similar diagram to panel (c) is shown in Hansen & Milosavljević (2003). The BBH loses energy mainly by interacting with stars when $t_{\text{gr}}(a_\bullet, \nu) > t_h(a_\bullet)$ and mainly by gravitational radiation when $t_{\text{gr}}(a_\bullet, \nu) < t_h(a_\bullet)$.

If we do not live at a special time, the lifetime of the BBH orbit, $\min(t_h, t_{\text{gr}})$, should exceed $\nu \times 10^{10} \text{ yr}$ (i.e. at most, the central BH should accrete a fraction ν of its mass in

a fraction ν of its age). This constraint is shown as the bold long-dashed line in panels (c) and (d) of Figure 2. We may combine this with the constraints from the position of Sgr A* (inequality 35), the near-Keplerian orbits of stars close to Sgr A*, and the proper motion of Sgr A* (inequalities 36–37), to conclude that the BBH should not be located in the dotted region in panel (d) of Figure 2. Note that we have assumed that M_1 coincides with Sgr A* and is the larger component of the BBH, so that ν cannot exceed 0.5 (eq. 32). However, if we relax this constraint, that is, if ν is allowed to exceed 0.5, we may extend the above constraints on the BBH parameter space and find that the forbidden region in Figure 2(d) excludes the range $0.5 < \nu < 1$. Thus, Sgr A* cannot be the smaller component of the BBH.

The bold dot-short-dashed line in Figure 2 (panels a and d) represents the semimajor axis at which the BBH becomes hard, given by equation (31). The average ejection velocity v_\bullet as a function of a_\bullet and ν is shown by short-dashed lines in these panels (these represent $v_\bullet = 400$ – 2000 km s^{-1} with interval $\delta v_\bullet = 200 \text{ km s}^{-1}$ from top to bottom, with $v_\bullet = 1000 \text{ km s}^{-1}$ shown in bold). Some short-dashed lines with $v_\bullet > 1000 \text{ km s}^{-1}$ cross the allowed region of panel (d), and hence there are allowed parameters for a BBH that could eject hypervelocity stars that reach the solar radius.

Thus, for example, consider a BBH with $\nu = 0.01$ and $a_\bullet = 0.5 \text{ mpc}$. This has orbital period $P_{\text{BBH}} \simeq 0.6 \text{ yr}$, gravitational radiation timescale $t_{\text{gr}} \simeq 4 \times 10^8 \text{ yr}$, and distance of Sgr A* from the center of mass of 0.1 mas , consistent with the observational constraints we have described. The time for a hypervelocity star to travel $D = 8 \text{ kpc}$ is $t_D \simeq 8 \times 10^6 \text{ yr} (D/8 \text{ kpc}) (10^3 \text{ km s}^{-1}/v_\bullet)$ (eq. 28). Since $t_D \ll \min(t_h, t_{\text{gr}})$, we can ignore the BBH orbital evolution, so the number of stars with ejection speed higher than 10^3 km s^{-1} within the sphere $D < 8 \text{ kpc}$ can be roughly estimated to be $n_{\text{BBH}}^{\text{diff}} t_D \simeq 10^3$.

4. Discussion and conclusions

We have studied stellar dynamical processes that eject hypervelocity ($> 10^3 \text{ km s}^{-1}$) stars from the Galactic center. We consider three mechanisms of ejecting stars: close encounters of two single stars, tidal breakup of binary stars, and three-body interactions between a star and a BBH.

The rate of ejection from close encounters of single stars is strongly affected by the finite size of stars: Figure 1 shows that this rate is 10^5 times smaller for solar-type stars than for point masses with the same radial distribution. For solar-type stars, the rate of ejection with speed $\gtrsim 10^3 \text{ km s}^{-1}$ at $R_0 = 8 \text{ kpc}$ is only 10^{-11} yr^{-1} , which is too low to be detectable. If there is a distribution of stellar masses, the ejection rate is likely to be larger for the lighter

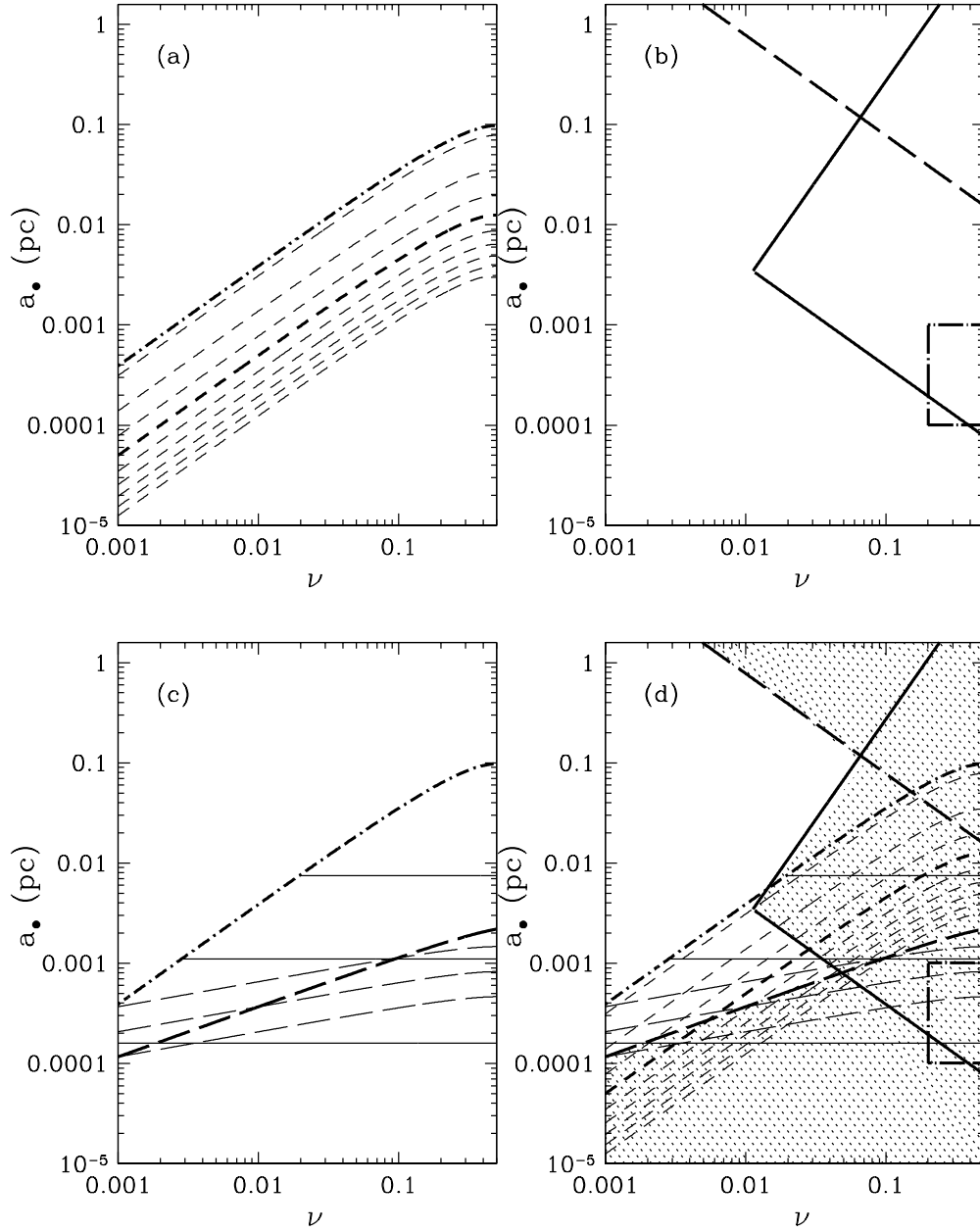


Fig. 2.— In each of the four panels, the horizontal axis represents the mass ratio $\nu \equiv M_2/(M_1 + M_2)$ of a hypothetical BBH in the Galactic center and the vertical axis represents its semimajor axis a_\bullet . Sgr A* is taken to be the more massive component of the BBH. The eccentricity of the BBH orbit is assumed to be zero. Panel (a): the bold dot-short-dashed line gives the semimajor axis of the BBH when it becomes hard (see eq. 31, with $\sigma_c = 100 \text{ km s}^{-1}$). The short-dashed lines represent the average ejection speeds of the stars from the BBH (eq. 33), $v_\bullet = 400\text{--}2000 \text{ km s}^{-1}$ from top to bottom with interval 200 km s^{-1} , with $v_\bullet = 1000 \text{ km s}^{-1}$ in bold. Panel (b): the region above the bold long-dashed line is the BBH parameter space that is excluded by the location of Sgr A* close to the center of the stellar cusp (see inequality 35). The rectangular region enclosed by the bold dot-long-dashed line is excluded by the Keplerian orbits of stars at radii $r \sim 0.1\text{--}1 \text{ mpc}$. The region on the right side of the bold solid line is excluded by the proper motion of Sgr A*, except for unusual orientations in which its motion is almost along the line of sight (inequalities 36 and 37). The kink at $a_\bullet \simeq 5 \text{ mpc}$ represents an approximate boundary between the cases in which the period of the BBH is long or short compared to the present duration of proper-motion observations. Panel (c): the long-dashed lines give the gravitational radiation timescale of the BBH: $10^9, 10^8, 10^7 \text{ yr}$ from top to bottom (eq. 39). The solid lines give the hardening time t_h : $4, 6, 8 \times 10^9 \text{ yr}$ from top to bottom (eq. 38). The region above the bold long-dashed line represents the constraint that $\min(t_h, t_{gr}) > \nu \times 10^{10} \text{ yr}$, so that the larger BH accretes at most a fraction ν of its mass in a fraction ν of its age (i.e. the present accretion rate of BH companions is not unusually large compared to the average over the lifetime of the Galaxy). As in panel (a), the bold dot-short-dashed line gives the semimajor axis of the BBH when it becomes hard. Panel (d): combination of the curves in panels (a)–(c). The shaded region is excluded. See §3.3.

stars (Hénon 1969), but these also have lower luminosity and thus are harder to detect.

The rate of ejection from breakup of binary stars (Hills 1988) depends on the orbital parameters of the binaries, such as the semimajor axis and component masses. We estimate that the rate of ejecting hypervelocity stars is $10^{-5}(\eta/0.1) \text{ yr}^{-1}$ (eq. 27), where η is the binary fraction and the result is only weakly dependent on semimajor axis for $a_b \lesssim 0.3 \text{ AU}$. This rate is also not strongly dependent on the stellar mass distribution. With the assumption that the binary components have the same mass m_* , the number of hypervelocity stars within the solar radius is ~ 100 for $\eta = 0.1$ and $a_b = 0.1 \text{ AU}$ (eq. 30).

Sgr A* may be one component of a BBH (Hansen & Milosavljević 2003). We discuss the constraints on the parameter space (mass ratio and semimajor axis) of the BBH using a variety of observational and theoretical arguments. The ejection speed of stars due to three-body interactions with the BBH depends on the BBH semimajor axis and mass ratio, but not on stellar mass. In part of the allowed parameter space, near $a_\bullet = 0.5 \text{ mpc}$ and $\nu = 0.01$, the average stellar ejection speed can exceed 10^3 km s^{-1} (see panel (d) of Fig. 2), and the rate of ejecting hypervelocity stars is $\sim 10^{-4} \text{ yr}^{-1}$. In this case the expected number of stars with ejection speeds higher than 10^3 km s^{-1} within the solar radius $r < 8 \text{ kpc}$ is $\sim 10^3$.

Nearby high-velocity halo stars bound to the Galaxy cannot have velocities that exceed the local escape speed. Recent estimates of the escape speed are $550 \pm 100 \text{ km s}^{-1}$ (Leonard & Tremaine 1990), $610 \pm 120 \text{ km s}^{-1}$ (Kochanek 1996), and 600 km s^{-1} (Wilkinson & Evans 1999), well below our cutoff at 10^3 km s^{-1} , so it is unlikely that bound halo stars can appear to be hypervelocity stars. Rare Local Group interlopers, perhaps from M31, could have velocities exceeding the escape speed. However, hypervelocity stars ejected from the Galactic center have an additional distinctive kinematic signature, since their velocity vectors should point almost directly away from the Galactic center (apart from small changes induced by the non-spherical component of the Galactic potential).

Hypervelocity stars produced at the Galactic center should also be distinguishable from runaway stars produced by supernova explosions in close binary systems or by close encounters in star clusters (Leonard 1993), which will have quite different velocity distributions.

At a distance of 10 kpc , a solar-type star traveling at 10^3 km s^{-1} has apparent magnitude $V = 19.8$ and proper motion 20 mas yr^{-1} . Ground-based surveys can achieve proper-motion accuracies of $\sim 1 \text{ mas yr}^{-1}$ with multiple images over baselines of a few years (Alard 2003). Planned ground-based surveys such as Pan-STARRS and the Large Synoptic Survey Telescope, with limiting magnitude $V \simeq 24$, could easily detect and measure the proper motion of solar-type hypervelocity stars over much of the Galaxy. The GAIA spacecraft will survey the whole sky to $V = 20$ with proper-motion accuracy of $\sim 0.1 \text{ mas yr}^{-1}$ or better at its

limiting magnitude.

In Hills’ mechanism, one component of the binary star is ejected, and the other is thrown onto a high-eccentricity orbit around the central BH (Gould & Quillen 2003). We expect that the number of young (10^7 yr old) stars that are the remnants of tidally disrupted binaries should be $\sim 100(\eta/0.1)$ at any time.

Hypervelocity stars produced by Hills’ mechanism should be approximately spherically distributed, while the spatial distribution of the hypervelocity stars due to interactions with the BBH should be flattened in the orbital plane of the BBH (see Zier & Biermann 2001).

Support for this research was provided in part by NASA through grants from the Space Telescope Science Institute, which is operated by the Association of Universities for Research in Astronomy under NASA contract NAS5-26555.

REFERENCES

- Alard, C. 2003, astro-ph/0306624
- Backer, D. C., & Sramek, R. A. 1999, ApJ, 524, 805
- Baganoff, F. K., et al. 2001, Nature, 413, 45
- Bahcall, J. N., & Wolf, R. A. 1976, ApJ, 208, 214
- Begelman, M. C., Blandford, R. D., & Rees, M. J. 1980, Nature, 287, 307
- Begelman, M. C., Blandford, R. D., & Rees, M. J. 1984, Rev. Mod. Phys., 56, 255
- Binney, J., & Tremaine, S. 1987, Galactic Dynamics (Princeton: Princeton University Press)
- Dehnen, W., & Binney, J. 1998, MNRAS, 294, 429
- Duquennoy, A., & Mayor, M. 1991, A&A, 248, 485
- Eisenhauer, F., et al. 2003, astro-ph/0306220
- Gebhardt, K., et al. 2003, ApJ, 583, 92
- Genzel, R., Pichon, C., Eckart, A., Gerhard, O. E., & Ott, T. 2000, MNRAS, 317, 348
- Genzel, R., Thatte, N., Krabbe, A., Kroker, H., & Tacconi-Garman, L. E. 1996, ApJ, 472, 153

- Genzel, R., et al. 2003, astro-ph/0305423
- Ghez, A. M., Klein, B. L., Morris, M., & Becklin, E. E. 1998, ApJ, 509, 678
- Ghez, A. M., Becklin, E., Duchene, G., Hornstein, S., Morris, M., Salim, S., & Tanner, A. 2003a, astro-ph/0303151
- Ghez, A. M., et al. 2003b, ApJ, 586, L127
- Ghez, A. M., et al. 2003c, astro-ph/0306130
- Gould, A., & Quillen, A. C. 2003, astro-ph/0302437, submitted to ApJ
- Hansen, B.M.S., & Milosavljević, M. 2003, astro-ph/0306074
- Hénon, M. 1960, Ann. d'Astrophys., 23, 467
- Hénon, M. 1969, A&A, 2, 151
- Hills, J. G. 1988, Nature, 331, 687
- Hills, J. G. 1991, AJ, 102, 704
- Kochanek, C. S. 1996, ApJ, 457, 228
- Komossa, S. 2003, in The Astrophysics of Gravitational Wave Sources, ed. J. Centrella (New York: American Institute of Physics), in press (astro-ph/0306439)
- Lin, D.N.C., & Tremaine, S. 1980, ApJ, 242, 789
- Leonard, P.J.T. 1993, in Luminous High-Latitude Stars, ed. D. D. Sasselov (San Francisco: ASP), 360
- Leonard, P.J.T., & Tremaine, S. 1990, ApJ, 353, 486
- Magorrian, J., & Tremaine, S. 1999, MNRAS, 309, 447
- Milosavljević, M., & Merritt, D. 2002, astro-ph/0212459
- Peters, P. C. 1964, Phys. Rev. B, 136, 1224
- Quinlan, G. D. 1996, New Astron., 1, 35
- Reid, M. J., Menten, K. M., Genzel, R., Ott, T., Schoedel, R., Eckart, A., & Brunthaler A. 2003, astro-ph/0304095

Reid, M. J., Readhead, A.C.S., Vermeulen, R. C., Treuhaft, R. N. 1999, ApJ, 524, 816

Schödel, R., et al. 2002, Nature, 419, 694

Schödel, R., et al. 2003, astro-ph/0306214

Volonteri, M., Haardt, F., & Madau, P. 2002, Ap&SS, 281, 501

Wilkinson, M. I., & Evans, N. W. 1999, MNRAS, 310, 645

Yu, Q. 2002, MNRAS, 331, 935

Zier, C., & Biermann, P. L. 2001, A&A, 377, 23